SUPPLEMENTARY MATERIAL

Supplementary Tables

Supplementary Table 1. Regions showing significant differences in functional connectivity with the NPS process (across the run; handholding runs>baseline runs)
(q<.05 FDR-corrected, gray matter mask)

Region/s	Peak coordinate	t-score	p-value
SI, R post-central gyrus	48, -20, 54	5.25	.00001
R PCC/precuneus	2, -57, 40	5.90	.000001
L PCC/precuneus	-7, -57, 38	4.14	.00036
L DMPFC	-5, 50, 16	3.90	.00070
R DMPFC	4, 57, 10	4.51	.00009
VMPFC	-7, 56, -4	4.24	.00020
R TPJ/ angular gyrus	49, -54, 16	4.37	.00051
L TPJ/supram./angular gyrus	-64, -49, 24	6.24	.0000008
Middle temporal gyrus	54, 4, -22	5.78	.000002
R Cerebellum	46, -47, -32	5.16	.000015
L Cerebellum	-38, -66, -38	4.24	.00020
L Ventral Striatum (Accumbens)	-7, 7, -8	4.18	.00024

SI, primary somatosensory cortex. R, right. L, left. PCC, posterior cingulate cortex. DMPFC, dorsomedial prefrontal cortex. VMPFC, ventromedial prefrontal cortex. TPJ, temporoparietal junction. Supram., supramarginal gyrus.

Supplementary Table 2. Path a, significant brain regions (q<.05 FDR-corrected, gray matter mask) showing pain-evoked activation reductions during handholding vs. baseline (positive values indicate pain activation reductions during handholding)

Region/s	Peak coordinate	z-stat (path a)	p-value
R DLPFC	46, 40, 20	4.55	.000005
L DLPFC	-48, 34, 16	5.01	.0000005
L precentral gyrus	-44, 2, 30	4.15	.00003
R OFC	34, 34, -16	4.05	.00005
L OFC	-32, 38, -20	3.94	.00007
OFC/gyrus rectus	-8, 36, -28	4.49	.000007
R MPFC	8, 44, 44	5.12	.0000003
L MPFC	-8, 40, 34	4.04	.00005

R ACC/paracingulate	2, 34, 30	4.85	.000001
L Insula	-34, 14, 4	4.05	.000049
SI/SII	62, -18, 32	4.39	.00001
PAG-brainstem	-6, -26, -6	4.44	.000008
L AMG-HFC	-24, -4, -24	4.11	.00004
Sup. Temporal gyrus/temporal pole	-48, 14, -20	4.82	.000001
	28, 10, -28	4.13	.00005
Inferior Temporal gyrus	30, 10, -44	3.97	.00007
L Caudate/Thalamus	-10, 2, 14	4.30	.00001
	-8, 8, 12	5.74	.000000009
Cerebellum	-42, -74, -50	4.33	.00001

SI, primary somatosensory cortex. R, right. L, left. PCC, posterior cingulate cortex. DMPFC, dorsomedial prefrontal cortex. VMPFC, ventromedial prefrontal cortex. TPJ, temporoparietal junction. Supram., supramarginal gyrus.

Supplementary Table 3. Path ab, Intensity model. Significant brain regions (q<.05 FDR-corrected, gray-matter mask) mediating pain intensity reductions during handholding (for path a, positive values indicate activation reductions during handholding; for path b, positive numbers indicate brain activation reductions that correlate with pain intensity reductions during handholding vs. baseline).

Region/s	Peak coordinate	Path ab z-stat /p-value	Path a z-stat /p-value	Path b z-stat / p-value
R DLPFC	32, 32, 28	4.06/.00001	1.06/.290	.02/.970
R VLPFC	32, 54, 8	4.03/.00005	.487/.626	-1.03/.302
Insula R	34, 30, 8	3.94/.00007	2.12/.033	-.02/.979
R VMPFC/DMPFC	8, 68, 8	4.18/.00002	.31/.759	-.69/.485
L VMPFC	-3, 67, -5	4.17/.00003	.99/.318	.60/.545
ACC/sup. frontal gyrus	-4, 36, 30	4.03/.00005	4.16/.00003	1.10/.270
Subgenual ACC	0, 14, -4	3.93/.00008	-.48/.626	-.77/.430
L OFC	-36, 36, -12	3.94/.00008	2.11/.034	.09/.924
L middle/inf. frontal gyrus	-28, 48, 6	4.03/.00005	-.16/.866	.11/.916
Brainstem/midbrain	6, -22, -18	4.26/.00002	1.42/.155	.92/.360
Parietal/angular gyrus	50, -58, 48	4.06/.00005	2.29/.021	2.72/.006
R middle/inf. temporal gyrus	62, -12, -30	4.17/.00003	2.37/.017	1.22/.219
R middle temporal gyrus	62, -32, -8	4.00/.00006	1.53/.126	.30/.766

R, right; L, left; DLPFC, dorsolateral prefrontal cortex; VLPFC, ventrolateral prefrontal cortex; VMPFC, ventromedial prefrontal cortex; DMPFC, dorsomedial prefrontal cortex; ACC, anterior cingulate cortex; sup., superior; OFC, orbitofrontal cortex; inf., inferior.

Supplementary Table 4. Path ab, Unpleasantness model. Significant brain regions (q<.05 FDR-corrected, gray-matter mask) mediating pain intensity reductions during handholding (for path a, positive values indicate activation reductions during handholding; for path b, positive numbers indicate brain activation reductions that correlate with pain intensity reductions during handholding vs. baseline).

Region/s	Peak coordinate	Path ab z-stat /p-value	Path a z-stat /p-value	Path b z-stat /p-value
ACC/SMA	-8, 12, 50	3.95/.00007	.634/.520	.157/.874
L DLPFC	-44, 36, 18	3.98/.00006	2.61/.008	1.27/.200
L DLPFC	-38, 36, 38	4.02/.00005	1.68/.092	.53/.592
R MPFC	6, 64, 16	3.99/.00006	1.52/.127	.38/.698
L MPFC	-2, 70, 8	4.30/.00001	1.10/.268	.99/.318
L OFC	-36, 38, -16	4.03/.00005	3.06/.002	2.24/.024
L Insula	-42, 8, -8	4.24/.00002	.60/.544	1.48/.138
Subgenual ACC	2, 34, -8	4.29/.00001	.22/.819	-1.09/.274
R DLPFC/VLPFC	32, 54, 8	3.95/.00007	.51/.605	-.290/.771
R middle temporal gyrus	62, -30, -12	4.12/.00003	1.75/.080	1.04/.294
L AMG	-18, 4, -30	4.00/.00006	3.59/.0003	1.04/.293
L middle occipital gyrus	-20, -86, -6	3.96/.00007	.23/.817	-.33/.735
Cerebellum	-16, -32, -22	4.20/.00002	-.19/.84	1.88/.059

ACC, anterior cingulate cortex; SMA, supplementary motor area; DLPFC, dorsolateral prefrontal cortex; MPFC, medial prefrontal cortex; OFC, orbitofrontal cortex; VLPFC, ventrolateral prefrontal cortex; AMG, amygdala.

Supplementary Table 5. Normalized dice coefficient table identifying similarity between handholding effects and cognitive demand (i.e., distraction) as measured using previously published working memory meta-analyses

	Handholding effects on pain			Working memory	
Network	Intensity a*b	Handholding Path a	Unpleas. a*b	WM meta 2003	Neurosynth RI
Visual	1	1	3	6	0
Somatomotor	0	3	0	8	0
dAttention	4	7	1	25	36
vAttention	14	9	10	10	11
Limbic	15	32	17	7	0
Frontoparietal	29	28	36	29	52
Default	38	20	34	15	1

Measure of the similarity between handholding effects and other manipulations of cognitive demand and attentional diversion, i.e., ‘distraction’, as measured using working memory meta-analyses. For the handholding effects

(Handholding path a, handholding vs. holding pneumatic device on brain activity during pain) and the mediation effect maps (a*b for intensity and unpleasantness), we calculated the similarity with each of the 7 major cortical networks in Yeo et al. 2011. We used a Dice coefficient metric, normalized across networks, to reflect the percentage of significant voxels in each map (FDR q < .05) that fell within each network. Path a: Normalized dice coefficients between significant brain regions (q<.05 FDR-corrected) in path a and each of the 7 networks in Yeo et al., 2011. Intensity a*b: Normalized dice coefficients between path a*b for the significant regions in the pain intensity model (q<.05 FDR-corrected) and each of the 7 networks in Yeo et al., 2011. Unpleasantness a*b: Normalized dice coefficients between path a*b for the significant regions in the pain unpleasantness model (q<.05 FDR-corrected) and each of the 7 networks in Yeo et al., 2011. WM meta 2003: Normalized dice coefficients between significant regions in the WM (working memory) meta-analysis (Wager and Smith, 2003) and each of the 7 networks in Yeo et al., 2011. Neurosynth RI: Normalized dice coefficients between Neurosynth RI ('reverse inference') map for the term working memory (Yarkoni et al. 2011) and each of the 7 networks in Yeo et al., 2011.

Supplementary Figures

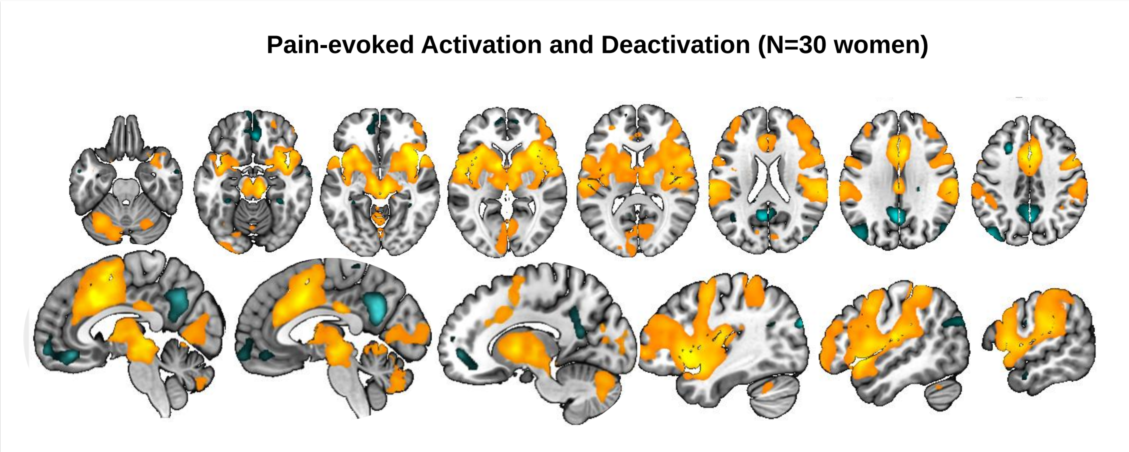

Supplementary Figure 1. Pain-evoked activation (warm colors) and deactivation (cold colors) during heat pain trials.

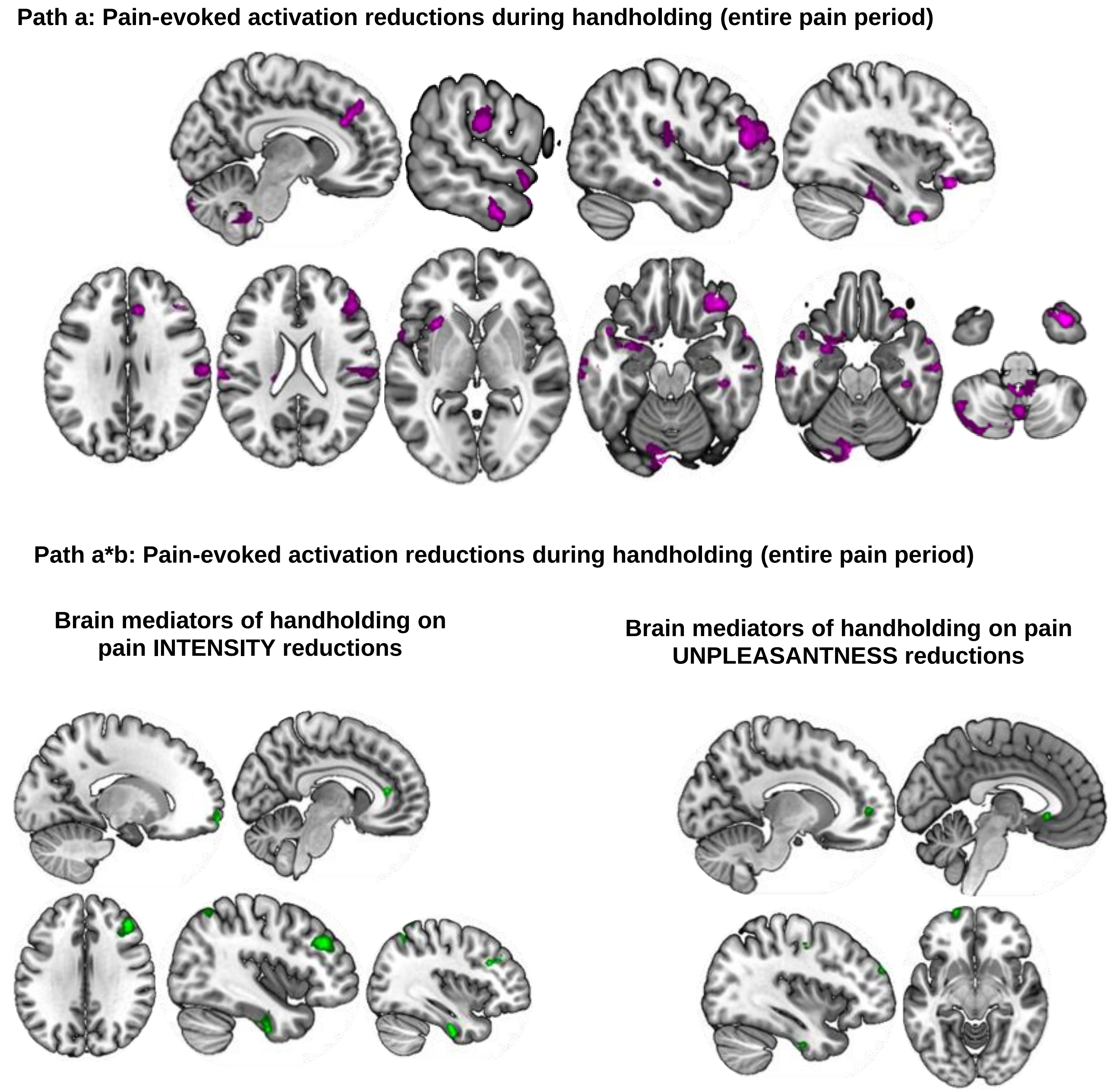

Supplementary Figure 2. Whole-brain multilevel mediation results (entire pain period). Upper panel. Illustration of Path *a* effects, i.e., effects of condition (handholding *vs.* baseline) on brain responses to pain (entire pain period). Brain image maps display brain activation reductions (p<0.001 uncorrected) in regions including DLPFC and ACC, medial prefrontal cortex, OFC, secondary somatosensory cortex, amygdala, temporal cortices and cerebellum. Lower panels. Brain mediators of handholding effects on pain intensity, i.e., greater pain-evoked brain activation reductions in these regions predict greater pain intensity reductions during handholding (p<0.001 uncorrected). **C.** Brain mediators of handholding effects on pain unpleasantness, i.e., greater pain-evoked brain activation reductions in these regions predict greater pain unpleasantness reductions during handholding (p<0.001 uncorrected).

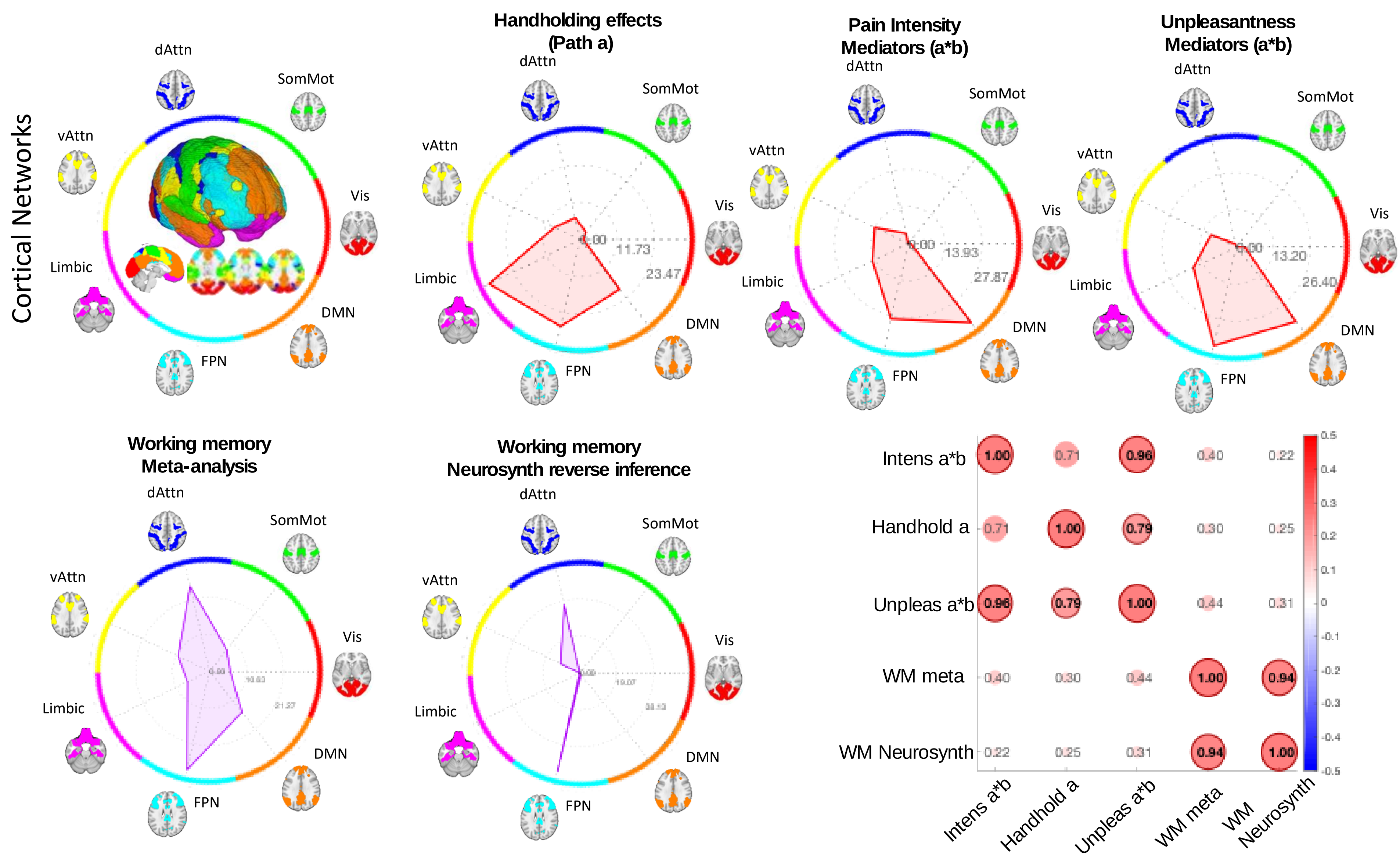
Cortical Networks
dAttn
SomMot
Vis
DMN
FPN
Limbic
vAttn
Handholding effects
(Path a)
0.00
11.73
23.47
Pain Intensity
Mediators (a*b)
13.93
27.87
Unpleasantness
Mediators (a*b)
13.20
26.40
Working memory
Meta-analysis
Working memory
Neurosynth reverse inference
Intens a*b
Handhold a
Unpleas a*b
WM meta
WM Neurosynth
1.00
0.71
0.96
0.40
0.22
0.79
0.30
0.25
0.44
0.31
0.94
0.5
0.4
0.3
0.2
0.1
0
-0.1
-0.2
-0.3
-0.4
-0.5

Supplementary Figure 3. Normalized dice coefficient representation using polar plots and a correlation matrix identifying similarity between handholding effects and cognitive demand (i.e., distraction) as measured using previously published working memory meta-analyses (Wager and Smith, 2003; Yarkoni et al., 2011). This study did not compare handholding to other strategies, but it is possible to compare the maps we identified of handholding effects on brain responses to pain to known patterns from other studies, to assess how similar handholding is to tasks that involve manipulation of cognitive demand. For the handholding effects (Path a, handholding vs. holding pneumatic device on brain activity during pain) and the mediation effect maps (a*b for intensity and unpleasantness), we calculated the similarity with each of the 7 major cortical networks in Yeo et al. 2011. We used a Dice coefficient metric, normalized across networks to reflect the percentage of significant voxels in each map (FDR $q < .05$) that fell within each network. These results are shown in the polar plots. We compared this with two meta-analyses of working memory (Wager and Smith, 2003 and Yarkoni et al., 2011), a widely studied cognitively demanding task that has shown some of the strongest 'distraction' effects on pain (Buhle and Wager, 2011; Sprenger and Buchel, 2015). Furthermore, to estimate the overall similarity between hand-holding and working memory across cortical networks, we calculated the correlation matrix across normalized Dice coefficients for all images reported in the. Correlation matrix.